DOI:10.1021/jf9017383

JOURNAL OF AGRICULTURAL AND FOOD CHEMISTRY
ARTICLE

Kinetic Analysis and Mechanism on the Inhibition of Chlorogenic Acid and Its Components against Porcine Pancreas α-Amylase Isozymes I and II

YUSAKU NARITA[†,‡] AND KUNIYO INOUYE*[,†]

[†]Division of Food Science and Biotechnology, Graduate School of Agriculture, Kyoto University, Sakyo-ku, Kyoto 606-8502, Japan, and [‡]R&D Center, UCC Ueshima Coffee Co, Ltd., 3-1-4 Zushi, Takatsuki-shi, Osaka 569-0036, Japan

Chlorogenic acid (5-caffeoylquinic acid, 5-CQA) is a kind of polyphenol and is richly included in green coffee beans. The inhibitory effects of 5-CQA and its components, caffeic acid (CA) and quinic acid (QA), on the two porcine pancreas α-amylase (PPA) isozymes, PPA-I and PPA-II, were investigated using *p*-nitrophenyl-α-D-maltoside as substrate at pH 6.9 and 30 °C. The inhibition potencies of the respective inhibitors against both PPA isozymes were almost the same and in the order of 5-CQA > CA ≫ QA. Their IC_{50} values were 0.07−0.08 mM, 0.37−0.40 mM, and 25.3−26.5 mM, respectively. The inhibition mechanisms of 5-CQA and CA were investigated by kinetic analyses, and the inhibitor constants K_i and K_i' (for the free enzyme and enzyme−substrate complex, respectively) were determined. It was indicated that 5-CQA and CA showed mixed-type inhibition with $K_i > K_i'$ against both PPA-I and PPA-II. The binding of PPA-I or PPA-II with 5-CQA or CA was all exothermic and enthalpy-driven. QA is a poor inhibitor, and its inhibitory mode was unique and hardly analyzed by a simple Michaelis−Menten-type interaction between the enzyme and inhibitor. However, it was shown that the inhibitory activity of CA was enhanced 5 times by ester-bond formation with QA in the form of 5-CQA. These results provide us with significant hints for the development of α-amylase inhibitors useful for the prevention of diabetes and obesity.

KEYWORDS: α-Amylase inhibitor; caffeic acid; chlorogenic acid; enzyme kinetics; mixed-type inhibition

INTRODUCTION

Chlorogenic acids (CGAs) refer to a family of esters between quinic acid and one or plural cinnamic acid derivatives such as caffeic, ferulic, and *p*-coumaric acids. They are richly contained in green coffee beans, and 34 kinds of CGAs were reported in green coffee beans (*1*, *2*). The contents of CGAs in green coffee beans are 3.5−7.5% (w/w-dry matter) for *Coffea arabica* and 7.0−14.0% (w/w-dry matter) for *Coffea canephora* (*3*, *4*). CGAs include three main classes which are caffeoylquinic acids, dicaffeoylquinic acids, and feruloylquinic acids (*3*, *4*). Their nomenclature is based on the IUPAC numbering system, and 5-caffeoylquinic acid (5-CQA) is generally called chlorogenic acid (*5*). The level of 5-CQA is more than 50% (w/w-dry matter) of total CGAs in green coffee beans (*3*, *4*). **Figure 1** shows the structures of 5-CQA and the components, caffeic acid (CA) and quinic acid (QA). CGAs are widely distributed in other plants such as yacon, burdock, prune, pear, potato, and sweet potato (*6*−*8*). Many investigators have reported that CGAs have various biological activities, such as antioxidant activity, antimutagenicity, suppression of cancer cells, melanin synthesis inhibition, matrix metalloproteinase inhibition, tyrosinase inhibition, virus-I integrase inhibition, DNA methylation inhibition, and so forth (*9*−*11*).

Porcine pancreas α-amylase (EC 3.2.1.1, hereafter abbreviated as PPA) is an endoglucanase that catalyzes the hydrolysis of α-1,4-glycosidic linkages in starch, amylose, amylopectin, and glycogen (*12*). PPA is composed of 496 amino acid residues and shows 83% homology with human pancreas α-amylase (*13*−*15*). Two active components were separated from a crystalline preparation of PPA in anion-exchange chromatography using DEAE-gels, and the component rapidly eluted was designated as PPA-1, and that slowly eluted was PPA-II (*16*, *20*). These isozymes are secreted in about equal amounts into pancreatic juice (*16*). The amino acid sequence of PPA-I is known (*15*, *17*), whereas only a partial amino acid sequence has been reported for PPA-II (*18*). PPA-I and PPA-II have almost the same molecular mass (*19*). The optimum pH values and temperatures for both isozymes in starch hydrolysis activity were similar and are 6.9 and 53 °C, respectively (*20*). Their isoelectric points are slightly different and are 6.5 and 6.1, respectively (*20*).

α-Amylase inhibitors seem to be effective for the prevention and therapy of metabolic syndromes such as type II diabetes and obesity in controlling the elevation of plasma blood glucose levels by delaying postprandial carbohydrate digestion and absorption. α-Amylase inhibitor from white beans (*Phaseolus vulgaris*) was

*To whom correspondence should be addressed. Tel: +81-75-753-6266. Fax: +81-75-753-6265. E-mail: inouye@kais.kyoto-u.ac.jp.

 Published on Web 09/16/2009

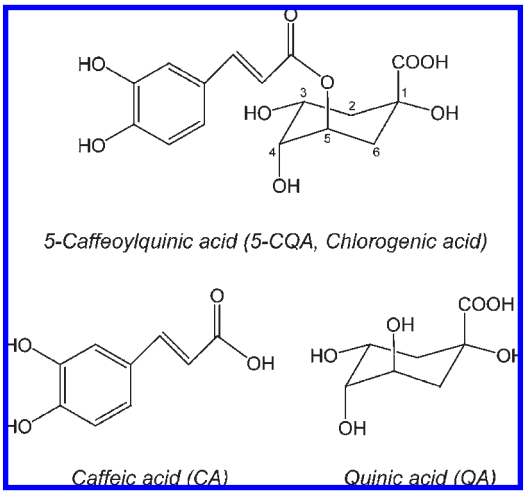

Figure 1. Structures of chlorogenic acid, caffeic acid, and quinic acid.

reported to reduce glycemia in both nondiabetic and diabetic animals and reduced the intake of food and water (*21*). α-Amylase inhibitor isolated from chestnut astringent skin extract was reported to suppress the rise in plasma glucose level after boiled-rice loading in a dose-dependent manner in humans (*22*). Various α-amylase inhibitors such as acarbose (*19*, *23*) and protein α-amylase inhibitor from wheat kernel (*24*) are discussed in the inhibition mechanism against PPA.

5-CQA, CA, and QA have already been reported to have inhibitory activity against commercially available crude PPA preparations in starch hydrolysis (*25*). However, the inhibitory activity against the purified PPA-I and PPA-II preparations has not yet been investigated. Furthermore, the inhibition mechanism has not been reported. In the present article, we describe the kinetic and thermodynamic analyses of the inhibitory effects of 5-CQA, CA, and QA on PPA-I and PPA-II activities and discuss their inhibitory mechanisms. We also provide some insights into the nutritional significance of the inhibitors and their preventive effects against diabetes and obesity.

MATERIALS AND METHODS

Materials. *p*-Nitrophenyl-α-D-maltoside (lot B76297-1, G_2-*p*NP) was purchased from Calbiochem (San Diego, CA). Pancreatin (lot M1P6865), chlorogenic acid hemihydrate (lot M7M4404), CA (lot M4F5063), D-(−)-QA (or QA, lot M5M5664), and all other chemicals were of reagent grade and were purchased from Nacalai Tesque (Kyoto, Japan).

Purification of PPA-I and PPA-II. PPA-I and PPA-II were purified according to the procedures previously reported (*24*) with some modifications. One gram of pancreatin was dissolved in 50 mL of 20 mM Tris-HCl buffer (pH 8.3, buffer A), to which 33 mL of chilled acetone was added, followed by centrifugation at 10,000*g* for 30 min at 4 °C. Acetone was further added to the supernatant to a final concentration of 67%, and the precipitates were collected by centrifugation. The precipitates were dissolved in buffer A and applied to anion-exchange HPLC on a TSKgel BioAssist Q column [10.0 mm (inner diameter) × 10.0 cm] (Tosoh, Tokyo, Japan) equilibrated with buffer A at 27 °C. A linear gradient was generated from 0 M to 50 mM NaCl at time 20.0 min over 40.0 min at a flow-rate of 1.0 mL/min. Absorption was measured with a Hitachi U-2910 spectrometer (Tokyo).

Sodium Dodecyl Sulfide−Polyacrylamide Gel Electrophoresis (SDS−PAGE) and Blue Native (BN)−PAGE. SDS−PAGE was carried out as follows according to the manual with the system and reagents supplied by Invitrogen (Carlsbad, CA). Protein samples were reduced by treatment with NuPAGE LDS sample buffer and NuPAGE reducing agent at 70 °C for 10 min. The samples were electrophoresed on a NuPAGE Novex 4−12% Bis-Tris gel with NuPAGE MES SDS running buffer in the Xcell *Surelock* Mini-Cell at 25 °C for 35 min at 200 V. Proteins were stained with Simplyblue safe stain buffer for 1 h, and their molecular weights were estimated using Novex Sharp Unstained Protein Standard (Invitrogen). BN−PAGE was also carried out with the system and reagents of Invitrogen. Protein samples were mixed with NativePAGE sample buffer, NativePAGE 5% G-250 sample additive, and 10% *n*-dodecyl-β-D-maltoside. The samples were electrophoresed on a NativePAGE 4−16% Bis-Tris gel in the Xcell *Surelock* Mini-Cell at 25 °C for 120 min at 150 V. The anode and cathode buffers were NativePAGE running buffer and that containing NativePAGE cathode buffer additive, respectively.

Hydrolysis of G_2-*p*NP by PPA. It is known that PPA hydrolyzes G_2-*p*NP at one position to produce *p*-nitrophenol (*p*NP) and maltose (*26*). Hydrolysis of G_2-*p*NP by 0.8 μM PPA (PPA-I or PPA-II) in 20 mM sodium phosphate buffer (pH 6.9, buffer B) containing 25 mM NaCl was measured continuously following the increase in absorbance at 400 nm due to *p*NP. The amount of *p*NP was evaluated using the molar absorption coefficient of 9.47 mM^{-1} cm^{-1} at pH 6.9 (*27*). The molecular activity (k_{cat}) and Michaelis constant (K_m) were calculated from Hanes−Woolf plots and Lineweaver−Burk plots (*28*, *29*).

Inhibition of PPA by 5-CQA, CA, and QA. Inhibitory activities of 5-CQA, CA, and QA against PPA were examined spectrophotometrically under the conditions used for the PPA activity measurement with G_2-*p*NP as substrate. Ten microliters of 40 μM PPA and 430 μL of various concentrations of the inhibitor ([5-CQA] = 0.0232−4.65 mM, [CA] = 0.116−4.65 mM, and [QA] = 5.81−11.6 mM) were mixed first and incubated for 30 min at a temperature of 20−40 °C. The hydrolysis was initiated by adding 60 μL of various concentrations (33.3−100.0 mM) of G_2-*p*NP to the enzyme−inhibitor mixture. The initial concentrations of PPA, 5-CQA, CA, QA, and G_2-*p*NP in the reaction mixture were 0.80 μM, 0.020−4.00 mM, 0.10−4.00 mM, 5.0−60.0 mM, and 4.0−12.0 mM, respectively. All measurements were performed in triplicate. Relative activity (%) in the presence of inhibitor was calculated by eq 1 using the initial velocities v_e and v_i in the absence and presence of the inhibitor, respectively.

$$\text{relative activity } (\%) = 100 \times (v_i/v_e) \quad (1)$$

The IC_{50} value was defined as the inhibitor concentration required for giving the relative activity of 50%. The type of inhibition was determined by Hanes−Woolf plots and Lineweaver−Burk plots. The inhibitor constants (K_i and K_i') were defined using the following general equation (eq 2) for mixed-type inhibition (*28*, *29*):

$$v_i = V_{max}[S]/\{K_m(1 + [I]/K_i)\} + \{[S](1 + [I]/K_i')\} \quad (2)$$

In eq 2, [S] and [I] are the initial concentrations of substrate and inhibitor, respectively; V_{max} is the maximum velocity observed under the conditions, $[S] \gg K_m$, in the absence of inhibitor; K_i is the inhibitor constant or the dissociation constant for the enzyme−inhibitor (EI) complex into the inhibitor (I) plus enzyme (E); and K_i' is that for the enzyme−substrate−inhibitor (ESI) complex into I plus the enzyme−substrate (ES) complex.

The standard enthalpy change (ΔH^o) for the binding of the enzyme (PPA-I and PPA-II) with the inhibitor (5-CQA and CA) was determined from the slope ($\Delta H^o/R$) of the plots of $1/K_i$ and $1/K_i'$ against $1/T$ (van't Hoff plots). The standard Gibbs energy change (ΔG^o) and standard entropy change (ΔS^o) for the binding of PPA with the inhibitor were determined according to the following equations:

$$\Delta G^o = -RT \ln(1/K_i) \text{ or } \Delta G^o = -RT \ln(1/K_i') \quad (3)$$

$$\Delta S^o = (\Delta H^o - \Delta G^o)/T \quad (4)$$

where R is the gas constant, and T is the temperature in Kelvin units. Hereafter, the thermodynamic parameters calculated based on K_i and K_i' were designated with the suffices of K_i and K_i', respectively, as ΔG^o_{Ki}, $\Delta G^o_{Ki'}$, and so forth.

RESULTS

Purification of PPA Isozymes. Two PPA fractions were eluted at 32.6 and 56.5 min in anion-exchange HPLC on a TSKgel BioAssist Q column. According to the nomenclature given

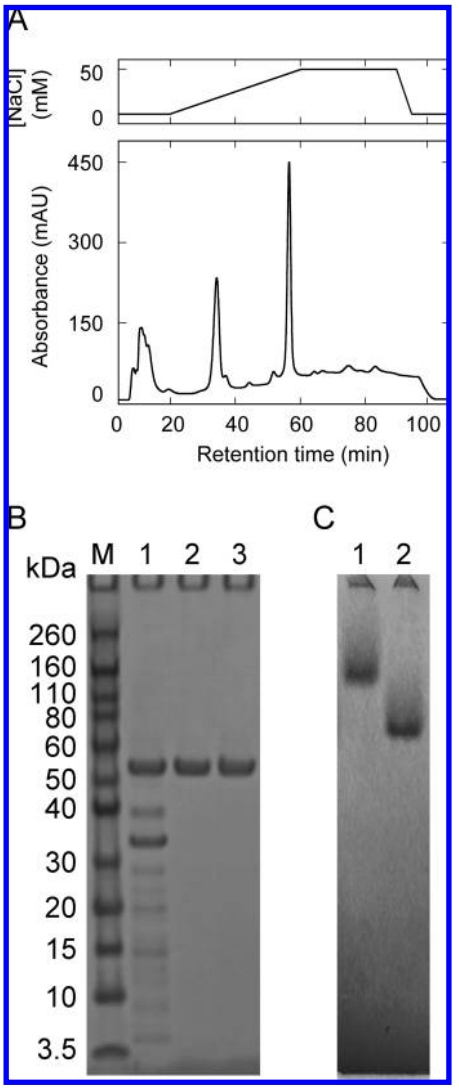

Figure 2. Purification of PPA-I and PPA-II by anion-exchange HPLC with TSKgel BioAssist Q and electrophoretic analyses of the purified PPA isozymes. (**Panel A**) A typical HPLC chromatogram of crude PPA (precipitates formed from pancreatin by 40−67% acetone). Fractions eluted around 32.6 and 56.5 min were collected as purified PPA-I and PPA-II preparations. (**Panel B**) SDS−PAGE of purified PPA-I and PPA-II. Lane M, molecular-weight markers (Novex Sharp Protein Standard, Invitrogen). Lane 1, crude PPA containing 7.5 μg protein; lane 2, purified PPA-I containing 5.0 μg protein; and lane 3, purified PPA-II containing 5.0 μg protein. (**Panel C**) BN−PAGE of purified PPA-I and PPA-II. Lane 1, purified PPA-I containing 5.0 μg protein and lane 2, purified PPA-II containing 5.0 μg protein. In SDS−PAGE and BN−PAGE, the cathode and anode were placed on the bottom and top sides of the PAGE plates, respectively.

previously (*16*, *20*), the respective fractions were assigned as PPA-I and PPA-II fractions (**Figure 2A**). The collected fractions were used for further analyses. Each of the PPA-I and PPA-II preparations showed a single band corresponding to 55.4 kDa on SDS−PAGE (**Figure 2B**) and also a single band on BN−PAGE (**Figure 2C**). The concentrations of PPA-I and PPA-II were determined using the molar absorption coefficient at 280 nm of 0.138 μM^{-1} cm^{-1} calculated using the molecular mass of 55.4 kDa and absorbance value at 280 nm ($A_{280,\,1\,cm} = 2.5$) and at the protein concentration of 1.0 mg/mL (*19*).

Inhibition of PPA by 5-CQA, CA, and QA. Figure 3 shows the inhibition by 5-CQA, CA, and QA of the PPA-I- and

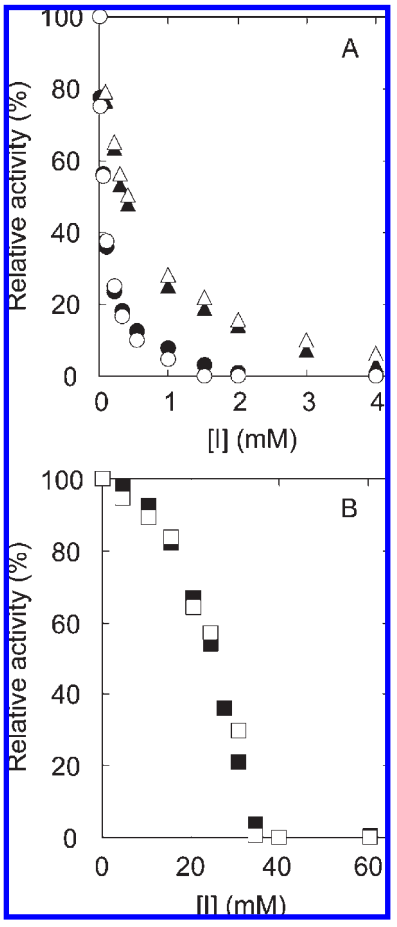

Figure 3. Inhibitory effects of 5-CQA, CA, and QA against PPA-I and PPA-II. PPA inhibitory activity assays were preformed in buffer B containing 25 mM NaCl at pH 6.9 and 30 °C. The initial concentration of PPA was 0.80 μM and that of G_2-*p*NP was 8.0 mM. The initial concentrations of 5-CA, CA, and QA were in the range of 0−4 mM, 0−4 mM, and 0−60 mM, respectively. (**Panel A**) Inhibition curves of 5-CQA against PPA-I activity (○), 5-CQA against PPA-II (●), CA against PPA-I (△), and CA against PPA-II (▲). (**Panel B**) Inhibition curves of QA against PPA-I activity (□) and QA against PPA-II (■). Each point represents the mean of triplicate experiments.

PPA-II-catalyzed hydrolysis of G_2-*p*NP at pH 6.9 and 30 °C. At the enzyme concentration of 0.80 μM and the substrate concentration of 8.0 mM, the v_e values of PPA-1 and PPA-II were determined to be 20.5 ± 1.3 and 23.1 ± 1.9 nM/s, respectively. The relative activities of PPA-I and PPA-II decreased with increasing 5-CQA concentration in a similar manner, and the IC_{50} values against PPA-I and PPA-II were 0.08 ± 0.02 and 0.07 ± 0.02 mM, respectively (**Figure 3A**). The complete inhibition of PPA-I was observed at 1.5 mM 5-CQA, and that of PPA-II was at 2.0 mM 5-CQA. The relative activities of PPA-I and PPA-II decreased also in a similar manner with increasing the CA concentration, and the IC_{50} values against PPA-I and PPA-II were 0.40 ± 0.03 and 0.37 ± 0.04 mM, respectively (**Figure 3A**). Almost all activities of PPA-I and PPA-II were lost in the presence of 4 mM CA. The curves showing the dependence of the relative activities of PPA-I and PPA-II on the QA concentration were substantially the same, although considerably different from those on the 5-CQA and CA concentrations (**Figure 3B**). The activities higher than 80% remained for both isozymes even in the presence of 15 mM QA, while they decreased sharply when the QA concentration increased from 15 to 35 mM. The IC_{50} values of QA against PPA-I and PPA-II were 26.5 ± 1.8 and

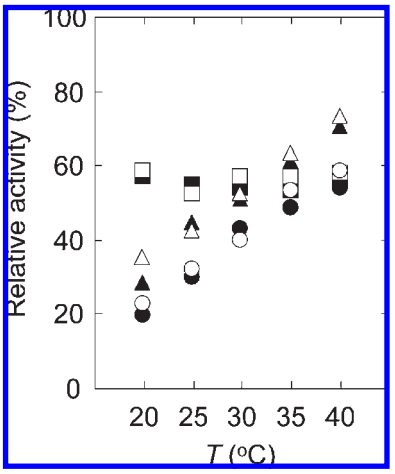

Figure 4. Temperature dependence of the inhibitory activity of 5-CQA, CA, and QA against PPA-I and PPA-II. PPA-I activity in the presence of 5-CQA (○), CA (△), and QA (□) were performed in buffer B containing 25 mM NaCl at pH 6.9 in the temperature range of 20−40 °C. The initial concentrations of PPA-I, G_2-*p*NP, 5-CQA, CA, and QA were 0.80 μM, 8.0 mM, 0.1 mM, 0.3 mM, and 25 mM, respectively. PPA-II activity in the presence of 5-CQA (●), CA (▲), and QA (■) were performed under the same conditions as those for PPA-I. Each point represents the mean of triplicate experiments.

25.3 ± 0.7 mM, respectively, and the complete inhibition of PPA-I was given with 35.0 mM QA, and that of PPA-II was with 40.0 mM QA. Comparing the IC_{50} values of 5-CQA, CA, and QA, the orders of the inhibitory activities of the inhibitors were the same for PPA-I and PPA-II and were 5-CQA > CA ≫ QA.

When Δv ($= v_e - v_i$) was plotted against the concentration of inhibitors, 5-CQA and CA, the curves of the plots were similar to a standard profile of Michaelis−Menten kinetics and the plots of [I]/Δv against [I] (Hanes−Woolf plots) and 1/Δv against 1/[I] (Lineweaver−Burk plots) gave straight lines (data not shown), indicating that each inhibitor binds stoichiometrically with each PPA isozyme at a molar ratio of 1:1. However, the dependence of Δv on QA concentration did not show Michaelis−Menten-type profiles for PPA-I and PPA-II (data not shown), suggesting that the inhibitory mechanism of QA against PPA might be unique and different from that of 5-CQA and CA.

Temperature Dependence of Inhibitory Activities of 5-CQA, CA, and QA. Figure 4 shows the inhibition of the PPA-catalyzed hydrolysis of G_2-*p*NP by 0.1 mM 5-CQA, 0.3 mM CA, and 25 mM QA at pH 6.9 in the temperature range of 20−40 °C. The relative activities of PPA-I and PPA-II in the presence of 0.1 mM 5-CQA or 0.3 mM CA increased linearly with increasing temperature. The activities of both isozymes were inhibited 80% at 20 °C and 40% at 40 °C by 0.1 mM 5-CQA; and 70% at 20 °C and 30% at 40 °C by 0.3 mM CA, suggesting that the inhibitory activities of 5-CQA and CA are dependent on the reaction temperature and that the lower the temperature is, the stronger their inhibitory activities are. It is interesting to note that the inhibition of PPA by QA was not dependent on temperature, and 40% of PPA-I and PPA-II activity was inhibited by 25 mM QA in the temperature range examined. These results suggested that the inhibitory mechanism of QA might be different from that of 5-CQA and CA as well as the results shown above (**Figure 3**).

Mixed-Type Inhibition of PPA-I and PPA-II by 5-CQA and CA. As the Michaelis−Menten kinetics was observed in the inhibition of PPA isozymes by 5-CQA and CA (cf. **Figure 3A**), the kinetics was examined more precisely. The initial velocity (v) was measured at 0.80 μM PPA-I and various concentrations (4−12 mM)

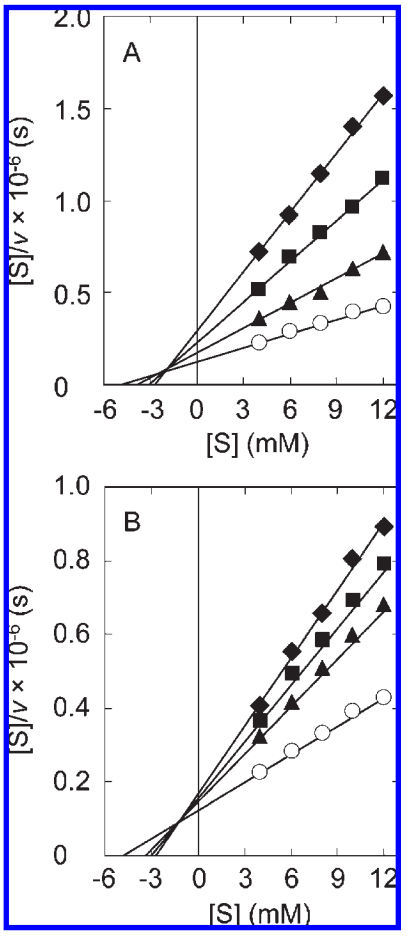

Figure 5. Hanes−Woolf plots for the PPA-I -catalyzed hydrolysis of G_2-*p*NP. PPA-I activity was measured in the presence of 5-CQA (**panel A**) and CA (**panel B**) under the same conditions as those shown in **Figure 2**. (**Panel A**) The 5-CQA concentration in the reaction mixture: 0 M (○), 50 μM (▲), 100 μM (■), and 200 μM (♦). (**Panel B**) The CA concentration in the reaction mixture: 0 M (○), 100 μM (▲), 200 μM (■), and 300 μM (♦). Each point represents the mean of triplicate measurements.

of G_2-*p*NP in the absence and presence of various concentrations of 5-CQA and CA at pH 6.9 and 30 °C. **Figure 5** shows the Hanes−Woolf plots for the PPA-I-catalyzed hydrolysis of G_2-*p*NP in the absence and presence of the inhibitors. The plots given at various inhibitor concentrations gave straight lines. The slope and intercept on the vertical axis of each line increased with increasing inhibitor concentration. The lines intersected each other on a point in the second quadrant, suggesting that the inhibition modes of 5-CQA and CA against PPA-I are mixed-type. The k_{cat} and K_m values for the PPA-I-catalyzed hydrolysis of G_2-*p*NP were determined to be (4.94 ± 0.23) × 10^{-2} s^{-1} and 4.48 ± 0.34 mM, respectively. The k_{cat} and K_m values in the presence of 100 μM 5-CQA were (1.52 ± 0.21) × 10^{-2} s^{-1} and 3.04 ± 0.32 mM, respectively, and those in the presence of 300 μM CA were (2.31 ± 0.21) × 10^{-2} s^{-1} and 3.04 ± 0.38 mM, respectively. The inhibitor constants, K_i and K_i', of 5-CQA and CA against PPA-I were calculated by eq 2. The respective values were 0.23 ± 0.02 mM and 0.05 ± 0.01 mM for 5-CQA and 1.12 ± 0.14 mM and 0.27 ± 0.04 mM for CA.

The inhibition kinetics was examined with PPA-II by 5-CQA and CA under the same conditions as those examined with PPA-I. The results obtained with PPA-II were similar to those with PPA-I (data not shown), suggesting that the inhibition modes of 5-CQA and CA against PPA-II are mixed-type too. The k_{cat}

and K_m values for the PPA-II-catalyzed hydrolysis of G_2-*p*NP were determined to be $(4.97 \pm 0.25) \times 10^{-2}$ s^{-1} and 4.63 ± 0.35 mM, respectively. The k_{cat} and K_m values in the presence of 100 μM 5-CQA were $(1.78 \pm 0.22) \times 10^{-2}$ s^{-1} and 3.12 ± 0.43 mM, respectively, and those in the presence of 300 μM CA were $(2.78 \pm 0.20) \times 10^{-2}$ s^{-1} and 3.32 ± 0.26 mM, respectively. The K_i and K_i' of 5-CQA against PPA-II were calculated to be 0.21 ± 0.02 mM and 0.05 ± 0.01 mM, respectively, and those of CA were 1.64 ± 0.30 mM and 0.25 ± 0.03 mM, respectively (**Table 1**).

The mixed-type inhibition suggests that there might be an inhibitor-binding site (or I-site) for 5-CQA and CA on the enzyme (PPA-I and PPA-II) surface in addition to the substrate-binding site (or S-site). It is noteworthy that the K_i' value is much lower than the K_i in all K_i and K_i' pairs, indicating that both 5-CQA and CA bind tighter to the I-site on the substrate-bound form of PPA-I and PPA-II than that on the free form. It is also noted that the K_m values in the presence of the inhibitors are lower than that in their absence. In other words, binding of the substrate to the S-site decreases the binding affinity of the inhibitor to the I-site, whereas binding of the inhibitor to the I-site increases the binding affinity of the substrate to the S-site.

Temperature Dependence of the Inhibitor Constants (K_i and K_i') of 5-CQA and CA. The van't Hoff plots of K_i and K_i' at pH 6.9 at temperatures of 20, 25, 30, 35, and 40 °C were examined (data not shown). From the slope of the plots, the standard enthalpy changes (ΔH^o) for the bindings of inhibitors (5-CQA and CA) with PPA isozymes were determined. The standard Gibbs energy changes (ΔG^o) and entropy changes (ΔS^o) at 25 °C were also calculated from eqs 3 and 4 (**Table 2**). These results indicated that the binding of PPA-I or PPA-II with 5-CQA or CA was accompanied with a large ΔH^o value, and thus the reaction was exothermic. It was shown that the binding was driven by a large increase in enthalpy (enthalpy-driven reaction). Enthalpy−entropy compensation was noticed in all cases.

DISCUSSION

Inhibitory Activities of 5-CQA, CA, and QA against PPA-I and PPA-II. The inhibitory activities of 5-CQA, CA, and QA against PPA-I and PPA-II were assayed with G_2-*p*NP substrate at pH 6.9 and 30 °C, and the inhibition potencies against both isozymes were evaluated to be in the order of 5-CQA > CA ≫ QA by comparing the IC_{50} values (**Table 1**). The inhibitory potencies of 5-CQA against two isozymes are similar, and those of CA and those of QA are also similar. In other words, these inhibitors do not discriminate the structural and functional differences between the isozymes. The inhibitory activities of 5-CQA, CA, and QA against PPA at pH 9 were reported using a starch substrate and a crude PPA preparation (the protein content in which was 53%; purchased from Fluka, Buchs, Switzerland), and the inhibition potencies were reported to be in the order of 5-CQA > CA > QA (*25*). This result agrees apparently with that obtained in the present article using PPA isozymes and a small synthetic substrate G_2-*p*NP, and the inhibitory potencies of 5-CQA, CA, and QA are likely to be similar to those of starch and G_2-*p*NP substrates. We have examined preliminarily the inhibition of PPA activity by the inhibitors in starch hydrolysis, although 60% of PPA activity remained even at excess inhibitor concentrations, such as 1 mM 5-CQA, suggesting that the inhibitory potency of the inhibitors might be weaker in the PPA-catalyzed hydrolysis of starch than that of G_2-*p*NP. We should point out the differences in the assay methods applied for PPA activity for starch and G_2-*p*NP. The reducing-activity measurement was applied to starch hydrolysis (*25*), but we have observed that it is strongly affected by carboxylic acids and sugar moieties of the inhibitors, although this point was not considered in the previous reports (*25*). Re-evaluation of the inhibitory potencies of 5-CQA, CA, and QA in the PPA-catalyzed hydrolysis of starch is currently underway with the development of a new assay method.

Although we have no direct evidence whether the three inhibitors interact with the same I-site or different ones on the enzyme surface, we propose a hypothetical model for the I-site on the basis of the IC_{50} values (**Table 1**) by mimicking the subsite structures demonstrated in the I-sites of proteinases (*30*−*33*). In this model, the three inhibitors bind to the same I-site which is separated into two subsites, CA and QA subsites. Here, we introduce a concept that the structure of 5-CQA is separated into CA and QA substructures, which are linked with an ester bond to form 5-CQA. CA and the CA substructure in 5-CQA could bind to the former subsite and QA and the QA substructure to the latter subsite. The interaction of CA with the CA subsite increases the inhibitory activity 70 times higher than that of QA with the QA subsite (**Table 1**). It was suggested that the CA substructure rather than the QA one may play a more significant role in the inhibitory activity of 5-CQA and that the inhibitory potency of CA is enhanced 5 times by combining with QA to form 5-CQA. In other words, there might be positive cooperativity between the interactions of CA and QA substructures with their respective subsites. It is interesting to note that the inhibitory potency of a metalloproteinase inhibitor, phosphoramidon [*N*-(α-L-rhamnopyranosyl-oxyhydroxyl-phosphophinyl)-L-Leu-L-Trp], against thermolysin is drastically enhanced when the rhamnopyranosyl substructure is removed, suggesting that there is negative coopreativity between the interaction of the rhamnopyranosyl substructure with the S1 subsite of the thermolysin active site and that of the remaining phosphoramidate substructure with the S1′-S2′ subsites (*34*, *35*).

The inhibitory mode of QA was unique and hardly analyzed with a simple Michaelis−Menten-type interaction between the

Table 1. Inhibitor Constants and IC_{50} of 5-CQA, CA, or QA against PPA-I or PPA-II[a]

enzyme	inhibitor	IC_{50} (mM)	K_i (mM)	K_i' (mM)
PPA-I	5-CQA	0.08 ± 0.02	0.23 ± 0.02	0.05 ± 0.01
	CA	0.40 ± 0.03	1.12 ± 0.14	0.27 ± 0.04
	QA	26.5 ± 1.8	NA[b]	NA
PPA-II	5-CQA	0.07 ± 0.02	0.21 ± 0.02	0.05 ± 0.01
	CA	0.37 ± 0.04	1.64 ± 0.30	0.25 ± 0.03
	QA	25.3 ± 0.7	NA	NA

[a] Each value is a mean of triplicate analysis ± standard deviation. [b] NA, samples not analyzed.

Table 2. Thermodynamic Parameters for the Interactions of 5-CQA or CA with PPA-I or PPA-II (Parameter Unit: kJ mol^{-1})[a]

enzyme	inhibitor	ΔG^o_{Ki}	$\Delta G^o_{Ki'}$	ΔH^o_{Ki}	$\Delta H^o_{Ki'}$	$T\Delta S^o_{Ki}$	$T\Delta S^o_{Ki'}$
PPA-I	5-CQA	−21.7 ± 1.7	−25.5 ± 1.9	−70.3 ± 4.3	−59.0 ± 3.6	−48.5 ± 3.9	−33.4 ± 3.7
	CA	−17.9 ± 2.5	−18.0 ± 2.6	−78.9 ± 6.2	−58.3 ± 5.9	−61.0 ± 6.0	−40.3 ± 5.8
PPA-II	5-CQA	−22.8 ± 2.3	−25.7 ± 2.5	−67.9 ± 9.3	−59.1 ± 6.1	−45.0 ± 8.9	−33.4 ± 5.9
	CA	−16.6 ± 1.7	−22.0 ± 2.1	−83.0 ± 4.4	−69.3 ± 4.1	−66.4 ± 4.2	−47.3 ± 3.9

[a] Each value is a mean of triplicate analysis ± standard deviation. ΔG^o and $T\Delta S^o$ values were given at 25 °C.

enzyme and inhibitor (**Figure 3B**). The inhibitory mode of QA must be examined further in the next research step kinetically and thermodynamically. Presently, as a matter of convenience, when it is assumed that PPA and QA interact at the ratio of 1:1 (mol/mol) and that the IC_{50} (26.5 mM) of QA against PPA gives an approximate K_i value, the ΔG^o for the interaction between PPA and QA was calculated by eq 3 to be -8.9 kJ mol^{-1} at 25 °C.

The ΔG^o values for the PPA-I inhibition by 5-CQA and CA are compared (**Table 2**). The contribution of CA is 83% in the ΔG^o_{Ki} value of 5-CQA, while it is 71% in the $\Delta G^o_{Ki'}$ value, suggesting that the substrate-binding to the S-site of PPA-I enhances the binding affinity of 5-CQA more than that of CA. Interestingly, the contribution of CA in the inhibition of PPA-II is 73% in the ΔG^o_{Ki} value, while it is 86% in the $\Delta G^o_{Ki'}$ value, suggesting that the substrate-binding to the S-site of PPA-II attenuates the binding affinity of 5-CQA more than that of CA. The inhibition of PPA-I by 5-CQA gives the ΔG^o_{Ki} value of -21.7 ± 1.7 kJ mol^{-1} and that by CA gives the value of -17.9 ± 2.5 kJ mol^{-1}, indicating that the QA substructure in 5-CQA might contribute to the ΔG^o_{Ki} value of 5-CQA by $\Delta\Delta G^o_{Ki}$ (QA) of -3.8 kJ mol^{-1}. The hypothetical contribution [$\Delta\Delta G^o_{Ki}$ (QA) or $\Delta\Delta G^o_{Ki'}$ (QA)] of the QA substructure in the binding affinity of 5-CQA to PPA was estimated likewise. The $\Delta\Delta G^o_{Ki'}$ (QA) value for PPA-I is -7.5 kJ mol^{-1}. For PPA-II, the $\Delta\Delta G^o_{Ki}$ (QA) and $\Delta\Delta G^o_{Ki'}$ (QA) are -6.2 and -3.7 kJ mol^{-1}, respectively. These results suggest that the QA substructure contributes more strongly to the interaction between 5-CQA and the PPA-I I-site when the S-site is accommodated with the substrate than when it is vacant, and inversely, the QA substructure contributes more strongly to the interaction between 5-CQA and the PPA-II I-site when the S-site is vacant than when it is accommodated with the substrate (*36*, *37*).

The $\Delta\Delta G^o_{Ki}$ (QA) and $\Delta\Delta G^o_{Ki'}$ (QA) values, which are considered to be measures of the contribution of the QA substructure in the interaction between 5-CQA and PPA isozymes, are in the range of $(-3.7)-(-7.5)$ kJ mol^{-1} (*32*, *33*). Although these values are lower than the ΔG^o value of -8.9 kJ mol^{-1} estimated from the PPA inhibition by QA, it could be safely stated that the binding affinity of 5-CQA to PPA was given roughly by the addition of those of CA and QA. This result supports our hypothetical model given above that the 5-CQA binding site on the PPA-I and PPA-II isozymes is composed of two subsites which accommodate the CA and QA substructures of 5-CQA, separately. We are currently examining the interaction between the inhibitors and PPA isozymes and also characterizing the I-site by fluoro-spectroscopic and surface-plasmon resonance spectroscopic analyses and chemical modification of the amino acid residues of PPA. The inhibitory activity of the CA plus QA mixture at various ratios and that of other CQA species such as 3-CQA, 4-CQA, 3,4-di-CQA, 3,5-diCQA, 3,4,5-triCQA, and 5-feruloyl-QA will be examined to further characterize the subsites for accommodating the CA and QA substructures.

Inhibititory Models of 5-CQA and CA against PPA-I and PPA-II. The dependence of Δv on the inhibitor (5-CQA and CA) concentration [I] shows a standard profile of the Michaelis–Menten-type kinetics. In addition, the linear relationship between [I]/Δv and [I] suggests that the enzyme (PPA-I and PPA-II) binds to each inhibitor (5-CQA or CA) at a molar ratio of 1:1. The inhibitory modes in all cases, namely, inhibition of PPA-I and PPA-II by 5-CQA and that by CA, were shown to be mixed-type inhibition (cf. **Figure 5**). In the general model for mixed-type inhibition (*29*, *36*, *37*), the ternary ESI complex formed with the enzyme (E), inhibitor (I), and substrate (S) is enzymatically active with a molecular activity of k'_{+2}, while the ES complex has that of k_{+2}. In the present study, both PPA isozymes were completely inhibited by 2 mM 5-CQA and by 4 mM CA (**Figure 3A**), indicating that the ESI complexes of the isozymes formed with 5-CQA or CA should not be active, or $k'_{+2} \ll k_{+2}$, although these rate constants were not determined, and the formation of the ESI complex as well as EI complex was not evidenced. These points will be investigated more precisely by rapid kinetics with the stopped-flow method and X-ray crystallographic analysis in the next step.

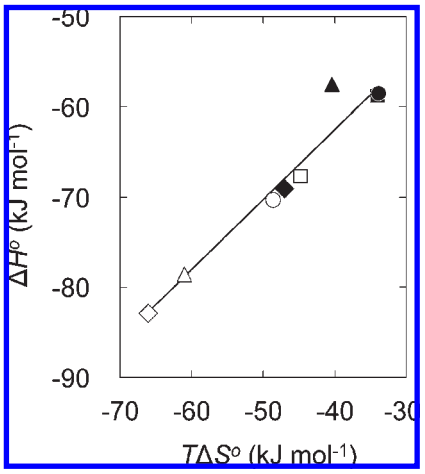

Figure 6. Relationship between the enthalpic changes (ΔH^o) and entropic changes ($T\Delta S^o$) for the interactions of the PPA isozymes (PPA-I and PPA-II) with 5-CQA and CA. The enthalpy–entropy compensation was indicated. The ΔH^o and $T\Delta S^o$ values derived from the K_i values are shown with open symbols, and those from the K_i' values are with closed ones. The interactions of PPA-I with 5-CQA and CA are shown with circles and triangles, respectively, and those of PPA-II with 5-CQA and CA are with squares and diamonds, respectively. The solid line was drawn by best fitting to the data. The slope of the line is 0.761 ± 0.070, and the correlation coefficient R is 0.976.

Thermodynamic Parameters for the Interactions of 5-CQA and CA with PPA-I and PPA-II. The ΔH^o value was determined from the slope of the van't Hoff plots in the temperature range of 20–40 °C. The ΔG^o and ΔS^o values at 25 °C were calculated using eqs 3 and 4 (**Table 2**). These results indicated that the interaction of PPA-I or PPA-II with 5-CQA or CA was exothermic and gave a large increase in ΔH^o, indicating that the interaction is enthalpy-driven. The plots were fitted to the regression line with a slope of 0.761 ± 0.070 (**Figure 6**). This value is close to the value of 1, and thus, the enthalpy–entropy compensation is noticed in all interactions of PPA isozymes with 5-CQA or CA. This type of compensation appears to be a widespread phenomenon and is widely invoked as an explanatory principle in thermodynamic analyses of proteins, ligands, and so forth. It has been suggested that this compensation is an intrinsic property of complex, fluctuating, or aqueous systems. When PPA and inhibitors interact to form EI complexes, the states of solvation of the enzyme and inhibitors might be changed accompanied with large changes in enthalpies and entropies, and thus with very little effect on the Gibbs energies of solvation (*38*–*40*).

Inhibitor Constants of 5-CQA and CA against PPA-I or PPA-II. The inhibitor constants K_i and K_i' that correspond to the dissociation constants K_d of the EI complex into I plus E and that of the ESI complex into I plus ES complex were determined from eq 2 (**Table 1**). It was indicated that both 5-CQA and CA showed mixed-type inhibition with $K_i > K_i'$, suggesting that the inhibitors bind to the ES complex stronger than to the enzyme. The inhibitor constants K_i and K_i' of acarbose, an antidiabetic drug, against PPA in the hydrolysis of maltopentaose at pH 6.9

and 30 °C were reported to be 3 μM and 0.62 μM, respectively (*41*). The K_i and K_i' values of 5-CQA against PPA-I in the hydrolysis of G_2-*p*NP are 0.23 ± 0.02 mM and 0.05 ± 0.01 mM, respectively. Acarbose is a potent α-amylase inhibitor, and its inhibitory activity is 100 times stronger than that of 5-CQA. 5-CQA may not be applicable for therapeutic use in humans because of its lower inhibitory activity in comparison with that of acarbose, but ingestion of 5-CQA from processed foods and beverages may be useful for the prevention of diabetes and obesity and for the management of borderline diabetes in patients.

ACKNOWLEDGMENT

We thank Dr. Seunjae Lee (Kyoto University and presently Samsung Everland, Ltd., Seoul) and R. Kimura and T. Fukunaga (UCC Ueshima Coffee Co.) for their valuable advice and fruitful comments.

LITERATURE CITED

(1) Clifford, M. N.; Kazi, T. The influence of coffee bean maturity on the content of chlorogenic acids, caffeine and trigonelline. *Food Chem.* **1987**, *26*, 59–69.

(2) Clifford, M. N.; Knight, S.; Surucu, B.; Kuhnert, N. T. Characterization by LC-MSn of four new classes of chlorogenic acid in green coffee beans: Dimethoxycinnamoylquinic acids, diferuloylquinic acids, and feruloyl-dimethoxycinnamoylquinic acids. *J. Agric. Food Chem.* **2006**, *54*, 1957–1969.

(3) Clifford, M. N. Chlorogenic acids and other cinnamates: Nature, occurrence and dietary burden. *J. Sci. Food Agric.* **1999**, *79*, 362–372.

(4) Ky, C.-L.; Louarn, J.; Dussert, S.; Guyot, B.; Hamon, S.; Noirot, M. Caffeine, trigonelline, chlorogenic acids and sucrose diversity in wild *Coffea arabica* L. and *C. canephora* P. accessions. *Food Chem.* **2001**, *75*, 223–230.

(5) IUPAC. Nomenclature of cyclitos. *Biochem. J.* **1976**, *153*, 23−31.

(6) Takenaka, M.; Yan, X.; Ono, H.; Yoshida, M.; Nagata, T.; Nakanishi, T. Caffeic acid derivatives in the roots of yacon (*Smallanthus sonchifolius*). *J. Agric. Food Chem.* **2003**, *51*, 793–796.

(7) Maruta, Y.; Kawabata, J.; Niki, R. Antioxidative caffeoylquinic acid derivatives in the roots of burdock (*Arctium lappa* L.). *J. Agric. Food Chem.* **1995**, *43*, 2592–2595.

(8) Islam, M. S.; Yoshimoto, M.; Yahara, S.; Okuno, S.; Ishiguro, K.; Yamakawa, O. Identification and characterization of foliar polyphenolic composition in sweetpotato (*Ipomoea batatas L.*) genotypes. *J. Agric. Food Chem.* **2002**, *50*, 3718–3722.

(9) Kono, Y.; Kobayashi, K.; Tagawa, S.; Adachi, K.; Ueda, A.; Sawa, Y.; Shibata, H. Antioxidant activity of polyphenolics in diets: Rate constants of reactions of chlorogenic acid and caffeic acid with reactive species of oxygen and nitrogen. *Biochim. Biophys. Acta* **1997**, *1335*, 335–342.

(10) Jin, U.-H.; Lee, J.-Y.; Kang, S.-K.; Kim, J.-K.; Park, W.-H.; Kim, J.-G.; Moon, S.-K.; Kim, A.-H. A phenolic compound, 5-caffeoylquinic acid (chlorogenic acid), is a new type and strong matrix metalloproteinase-9 inhibitor: Isolation and identification from methanol extract of *Euonymus alatus*. *Life Sci.* **2005**, *77*, 2760–2769.

(11) Iwai, K.; Kishimoto, N.; Kakino, Y.; Mochida, K.; Fujita, T. *In vitro* antioxidative effects and tyrosinase inhibitory activities of seven hydroxycinnamoyl derivatives in green coffee beans. *J. Agric. Food Chem.* **2004**, *52*, 4893–4898.

(12) Robyt, J. F.; French, D. The action pattern of porcine pancreatic α-amylase in relationship to the substrate binding site of the enzyme. *J. Biol. Chem.* **1970**, *245*, 3917–3927.

(13) Nakamura, Y.; Ogawa, M.; Nishida, T.; Emi, M.; Kosaki, G.; Himeno, S.; Matsubara, K. Sequences of cDNAs for human salivary and pancreatic α-amylase. *Gene* **1984**, *28*, 263–270.

(14) Nishida, T.; Nakamura, Y.; Mitsuru, E.; Yamamoto, T.; Ogawa, M.; Mori, T.; Matsubara, K. Primary structure of human salivary α-amylase gene. *Gene* **1986**, *41*, 299–304.

(15) Pasero, L.; Mazzei-Pierron, Y.; Abadie, B.; Chicheportiche, Y.; Marchis-Mouren, G. Complete amino acid sequence and location of the five disulfide bridges in porcine pancreatic α-amylase. *Biochim. Biophys. Acta* **1986**, *869*, 147–157.

(16) Marchis-Mouren, G.; Pasero, L. Isolation of two amylases in porcine pancreas. *Biochim. Biophys. Acta* **1967**, *140*, 366–368.

(17) Kluh, I. Amino acid sequence of hog pancreatic α-amylase isoenzyme I. *FEBS Lett.* **1981**, *136*, 231–234.

(18) Meloun, B.; Kluh, I.; Moravek, L. Hog pancreatic α-amylase. Peptides from tryptic digest of isoenzyme AII. *Collect. Czech. Chem. Commun.* **1980**, *45*, 2572–2582.

(19) Al Kazaz, M.; Desseaux, V.; Marchis-Mouren, G.; Payan, F.; Forest, E; Santimone, M. The mechanism of porcine pancreatic α-amylase: Kinetic evidence for two additional carbohydrate binding sites. *Eur. J. Biochem.* **1996**, *241*, 787–796.

(20) Sakano, Y.; Takahashi, S.; Kobayashi, T. Purification and properties of two active components from crystalline preparation of porcine pancreatic α-amylase. *J. Jpn. Soc. Starch Sci.* **1983**, *30*, 30–37.

(21) Tormo, M. A.; Gil-Exojo, I.; Romero de Tejada, A.; Campillo, J. E. White bean amylase inhibitor administered orally reduces glycemia in type 2 diabetic rats. *Br. J. Nutr.* **2006**, *96*, 539–544.

(22) Tsujita, T.; Yakaku, T.; Suzuki, T. Chestnut astringent skin extract, an α-amylase inhibitor, retards carbohydrate absorption in rats and humans. *J. Nutr. Sci. Vitaminol.* **2008**, *54*, 82–88.

(23) Al Kazaz, M.; Desseaux, V.; Marchis-Mouren, G.; Prodanov, E.; Santimone, M. The mechanism of porcine pancreatic α-amylase: Inhibition of maltopentaose hydrolysis by acarbose, maltose and maltotriose. *Eur. J. Biochem.* **1998**, *252*, 100–107.

(24) Oneda, H.; Lee, S.; Inouye, K. Inhibitory effect of 0.19 α-amylase inhibitor from wheat kernel on the activity of porcine pancreas α-amylase and its thermal stability. *J. Biochem.* **2004**, *135*, 421–427.

(25) Rohn, S.; Rawel, H. M.; Kroll, J. Inhibitory effects of plant phenols on the activity of selected enzymes. *J. Agric. Food Chem.* **2002**, *50*, 3566–3571.

(26) Levitzki, A.; Steer, M. L. The allosteric activation of mammalian alpha-amylase by chloride. *Eur. J. Biochem.* **1974**, *41*, 171–180.

(27) Yamashita, H.; Nakatani, H.; Tonomura, B. Substrate-selective activation of histidine-modified porcine pancreatic α-amylase by chloride ion. *J. Biochem.* **1991**, *110*, 605–607.

(28) Segel, I. H. Rapid Equilibrium Partial and Mixed-Type Inhibition. In *Enzyme Kinetics*; John Wiley & Sons: New York, 1975; pp 161−226.

(29) Cornish-Bowden, A. A simple graphical method for determining the inhibition constants of mixed, uncompetitive and non-competitive inhibitors. *Biochem. J.* **1974**, *137*, 143–144.

(30) Inouye, K.; Lee, S.-B.; Tonomura, B. Effects of amino acid residues at the cleavable site of substrates on the remarkable activation of thermolysin by salts. *Biochem. J.* **1996**, *315*, 133–138.

(31) Inouye, K.; Kuzuya, K.; Tonomura, B. A spectrophotometric study on the interaction of thermolysin with chloride and bromide ions, and the states of tryptophyl residue 115. *J. Biochem.* **1994**, *116*, 530–535.

(32) Muta, Y.; Inouye, K. Inhibitory effects of alcohols on thermolysin activity as examined using a fluorescent substrate. *J. Biochem.* **2002**, *132*, 945–951.

(33) Oneda, H.; Inouye, K. Interactions of human matrix metalloproteinase 7 (matrilysin) with the inhibitors thiorphan and R-94138. *J. Biochem.* **2001**, *129*, 429–435.

(34) Komiyama, T.; Suda, H.; Aoyagi, T.; Takeuchi, T.; Umezawa, H.; Fujimoto, K.; Umezawa, S. S. Studies on inhibitory effect of phosphoramidon and its analogs on thermolysin. *Arch. Biochem. Biophys.* **1975**, *171*, 727–731.

(35) Tronrud, D. E.; Monzingo, A. F.; Matthews, B. W. Crystallographic structural analysis of phosphoramidates as inhibitors and transition-state analogs of thermolysin. *Eur. J. Biochem.* **1986**, *157*, 261–268.

(36) Cornish-Bowden, A. Inhibitors and Activators. In *Principles of Enzyme Kinetics*; Butterworths: London, 1976; pp 52−70.

(37) Oneda, H.; Shiihara, M.; Inouye, K. Inhibitory effects of green tea catechins on the activity of human matrix metalloproteinases 7 (matrilysin). *J. Biochem.* **2003**, *133*, 571–576.

(38) Jencks, W. P. Strain, Distortion, and Conformation Change. In *Catalysis in Chemistry and Enzymology*; McGraw-Hill: New York, 1969; pp 282−320.
(39) Sharp, K. Entropy-enthalpy compensation: Fact or artifact? *Protein Sci*. **2001**, *10*, 661–667.
(40) Cornish-Bowden, A. Enthalpy-entropy compensation: a phantom phenomenon. *J. Biosci*. **2002**, *27*, 121–126.
(41) Desseaux, V.; Koukiekolo, R.; Moreau, Y.; Santimore, M.; Marchis-Mouren, G. Mechanism of porcine pancreatic α-amylase: inhibition of amylase and maltopentaose hydrolysis by various inhibitors. *Biologia* (*Bratislava*) **2002**, *57*, 163–170.

Received May 23, 2009. Revised manuscript received August 13, 2009. Accepted August 26, 2009. This study was supported in part by the Grants-in-Aid for Scientific Research (nos. 17380065 and 20380061) from the Japan Society for the Promotion of Science.